# 'Green' derivatization of carbon nanotubes with Nylon 6 and L-alanine

**Vladimir A. Basiuk,*[a] Carolina Salvador-Morales,[be] Elena V. Basiuk,[c] Robert M. J. Jacobs,[d] Michael Ward,[b] Bryan T. Chu,[b] Robert B. Sim[e] and Malcolm L. H. Green[b]**

***Received 10th August 2006, Accepted 5th September 2006***
***First published as an Advance Article on the web 25th September 2006***
**DOI: 10.1039/b611562d**

Amide derivatives of L-alanine and ε-caprolactam were readily obtained on diamine-functionalized oxidized single-walled and pristine multi-walled carbon nanotubes through a one-step direct amidation reaction, which employs thermal activation at 160–200 °C instead of chemical activation, avoids the use of organic solvents, and requires a few hours only for completion. In the case of ε-caprolactam, amino groups attached to the nanotubes initiated polymerization into Nylon 6. The functionalized nanotubes were characterized by infrared and Raman spectroscopy, scanning and transmission electron microscopy, atomic force microscopy, thermal gravimetric analysis and differential scanning calorimetry.



## 1. Introduction

The global trend of looking for environmentally friendly 'green' techniques in chemistry has rapidly and inevitably expanded to the chemical modification of carbon nanotubes (CNTs). An especially important issue is avoiding the use, or at least reducing the consumption of organic solvents in related chemical processes. During the last few years, significant improvements have been achieved in this area. A number of reports appeared on the design of simple and efficient solvent-free approaches to the covalent chemical modification of CNTs, which reflect different aspects of nanotube chemistry. For example, fluorination of single-walled CNTs (SWNTs)[1–3] and their functionalization with diazonium salts[4,5] rely basically upon the chemistry of the entire ideal nanotube sidewalls. By contrast, the direct amidation of oxidized SWNTs[6–8] represents the chemistry of carboxylic functionalities located mainly on the ends of acid-oxidized nanotubes. Two most recent examples of the solvent-free functionalization reactions are the amine[9,10] and thiol[11,12] nucleophilic addition to the defects of pristine MWNTs. In this case, we believe that the reactive sites are mainly pentagonal defects of the nanotube sidewalls (causing 'kinking') and closed ends, as supported by the results of quantum-chemical calculations,[9,12,13] although the existence of other types of reactive defects cannot be discarded.

The known examples of CNT chemical modification in the gas phase employ fluorine gas[1–3] or relatively volatile, simple organic compounds such as amines[6,9,10] and thiols.[11,12] Nevertheless, the variety of potential functionalizing reagents can be dramatically expanded to compounds which are non-volatile at room temperature and atmospheric pressure, if reduced pressure (vacuum) and elevated temperature (*e.g.*, above 100 °C) are employed simultaneously. The viability and efficiency of this approach has already been demonstrated in the surface modification of silica materials. More than a decade ago, we performed systematic studies on the use of the gas-phase chemical derivatization for the synthesis of chemically modified silicas, mainly as stationary phases for liquid-chromatography.[14–18] Among the derivatizing reagents tested were polyazamacrocyclic ligands,[14,16] pyrimidine bases,[16,18] and solid carboxylic acids.[15,17] In all of the above cases, decreasing the pressure to a moderate vacuum and simultaneously increasing the temperature to >150 °C resulted in efficient formation of the chemically bonded surface-groups. In particular, the direct amidation reaction between silica-bonded aminopropyl groups and vaporized carboxylic acids proceeds smoothly at 150–180 °C without any chemical activation of the carboxylic groups; a short (0.5–1 h) treatment is sufficient to provide high yields of the amide derivatives, in excess of 50% based on the starting surface concentration of aminoalkyl groups. In addition, excess derivatizing reagent is spontaneously removed from the reaction zone, thus making washing out and other auxiliary steps unnecessary. It was these observations which prompted us to adopt this method for the direct amidation of oxidized SWNTs,[6,7] although the location of reacting groups was inverted: the COOH groups were attached to the nanotubes, and the gas-phase reagent was an amine.

Amino acids and their derivatives are important examples of carboxylic acids. Their chemical attachment to CNTs is of significant academic and practical interest, since it not only improves the nanotube solubility[19] (including that in aqueous medium), but also opens a broad prospect for their biomedical applications.[20–22] Solid amino acids exist as zwitterions and therefore are not volatile compounds, however, reducing the pressure to a moderate vacuum of *ca.* $10^{-1}$ Torr makes many of them (including bifunctional α-amino acids) sublime above 150 °C without noticeable decomposition,[23] as well as enabling studies of interesting condensation reactions of their gas-phase

[a]*Instituto de Ciencias Nucleares, Universidad Nacional Autònoma de Mèxico (UNAM), Circuito Exterior C.U., 04510 Mèxico D.F., Mexico. E-mail: basiuk@nucleares.unam.mx.*
[b]*Inorganic Chemistry Laboratory, University of Oxford, South Parks Road, Oxford, OX1 3QR, U.K.*
[c]*Centro de Ciencias Aplicadas y Desarrollo Tecnològico, UNAM, Circuito Exterior C.U., 04510 Mèxico D.F., Mexico*
[d]*Chemistry Research Laboratory, University of Oxford, Mansfield Road, Oxford, OX1 3TA, U.K.*
[e]*Department of Biochemistry, University of Oxford, South Parks Road, Oxford, OX1 3QU, U.K.*

 

species.[24–29] These species keep an intramolecular association between the amino and carboxylic functionalities (much less polarized than in the zwitterions), but at the same time can form peptide bonds with amino acid moieties bound to solid surfaces (*e.g.*, silica).[24–29]

Furthermore, a number of important synthetic polymers are based on long-chain amino acids. The most illustrative example is Nylon 6, a polymer of ε-aminocaproic acid. CNT/Nylon hybrids recently attracted the attention of several research groups due to the possibility of obtaining new nanocomposites of remarkable mechanical strength[30–33] and better biocompatibility.[34] Two general approaches to prepare such nanocomposites are simple melt compounding[30,31,34] and ring-opening polymerization from the CNT surface.[32,33] In the latter case, ε-caprolactam is used as the monomer, whose polymerization on the nanotubes (oxidized SWNTs in both studies) in melt has to be initiated by adding sodium metal as a strong base,[33] or by being carried out at temperatures as high as 250 °C.[32]

ε-Caprolactam has an even greater volatility than that of amino acids; it melts at 68–71 °C, and its boiling point is 136–138 °C at 10 Torr. Therefore it satisfies the general criteria for a gas-phase derivatization reagent. Accordingly, one of the goals of the present research was to test the possibility of gas-phase derivatization of amino-functionalized CNTs with ε-caprolactam. As the amino-functionalized CNTs, we used oxidized SWNTs ($SWNT_{ox}$, Scheme 1) converted into amide derivatives $SWNT_{ox}18$ through gas-phase treatment[6,7] with 1,8-diaminooctane, as well as pristine MWNTs having numerous sidewall defects, treated with the same diamine (MWNT18) in the gas phase.[9,10] We expected ε-caprolactam to undergo ring-opening and form an amide with the second amino group of 1,8-diaminooctane, with the possibility of further polymerization producing Nylon 6 oligomer/polymer ($SWNT_{ox}18C$ and MWNT18C, Scheme 1). Another goal was to perform a similar study of L-alanine (Ala; representing simple bifunctional α-amino acids) interaction with the same $SWNT_{ox}18$ and MWNT18 nanotubes; in this case we were looking for evidence of amide attachment, producing the derivatized nanotubes $SWNT_{ox}18A$ and MWNT18A.

## 2. Results and discussion

In order to covalently modify $SWNT_{ox}$ and pristine MWNTs with 1,8-diaminooctane, we employed two different kinds of the nanotube chemistry, depending on the location of the

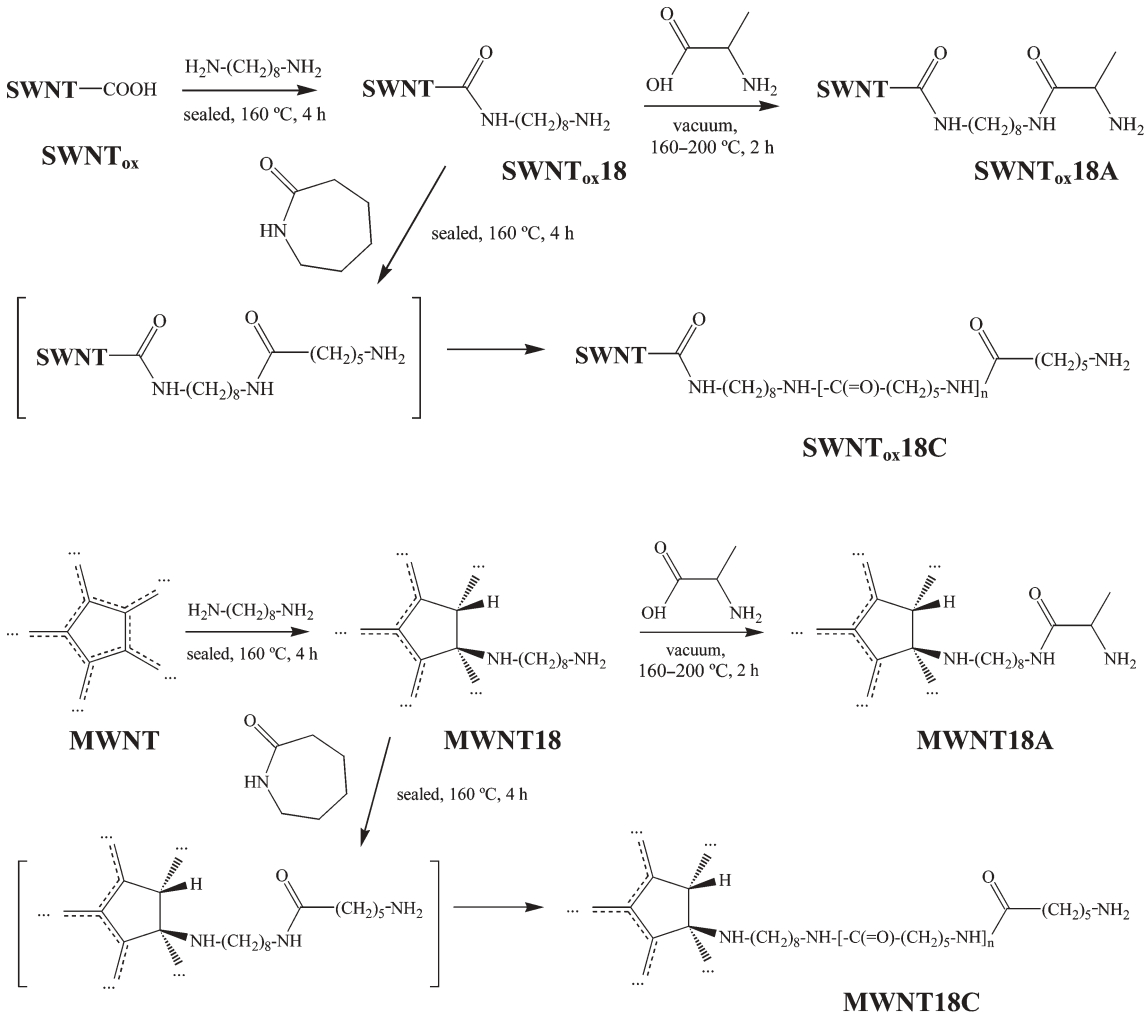


**Scheme 1** Chemical attachment of 1,8-diaminooctane to $SWNT_{ox}$ and MWNTs and further derivatization reactions with L-alanine and ε-caprolactam.

reactive sites. In the case of $SWNT_{ox}$, we used the direct thermal amidation reaction,[6–8] which involves the chemistry of carboxylic functionalities located mainly on the nanotube ends (Scheme 1). Pristine MWNTs were functionalized through the nucleophilic addition of amine groups[9,10] to the nanotube defects. We believe that the reactive sites are mainly pentagonal defects in the sidewalls and closed ends (which was supported by quantum-chemical calculations[9,12,13]), although we cannot discard the existence of other types of reactive defects. Raman spectra of the MWNTs used in our study exhibit a typical disorder band at 1343 $cm^{-1}$, whose intensity is comparable to that for a G-band at 1575 $cm^{-1}$, and therefore the density of defects in the nanotube samples is high. No reliable change in the D/G band ratio was observed in the Raman spectra of 1,8-diaminooctane-functionalized MWNTs (MWNT18, Scheme 1).

All of the functional groups which we attempted to attach to CNTs are polar. Therefore the first indication of successful modification reactions could be an improved solubility or dispersibility in polar solvent. We tested this by means of a short period of ultrasonication (5 min) in isopropanol; the images 15 min after the sonication are shown in Fig. 1. The modified SWNT samples produced a slight yellow–brown coloration of the solution phase; nevertheless, the nanotubes began to precipitate after less than one hour. The suspensions of the functionalized MWNT samples were even less stable (although more stable than that of pristine MWNTs), and no visible coloration of the isopropanol phase was observed.

FTIR spectra (Fig. 2 and Fig. 3) revealed the features which were expected. The bands most typical for CNT-bound organic moieties correspond to C–H bending (1360–1470 $cm^{-1}$) and C–H stretching vibrations (2850–2930 $cm^{-1}$). In addition, the C=O stretching ('amide I') absorption at 1630–1650 $cm^{-1}$ and N–H bending ('amide II') bands at 1550–1580 $cm^{-1}$ are indicative of the successful derivatization reactions. A weak diffuse absorption around 3300 $cm^{-1}$ ,due to N–H stretching vibrations, was barely seen for the SWNT-based samples

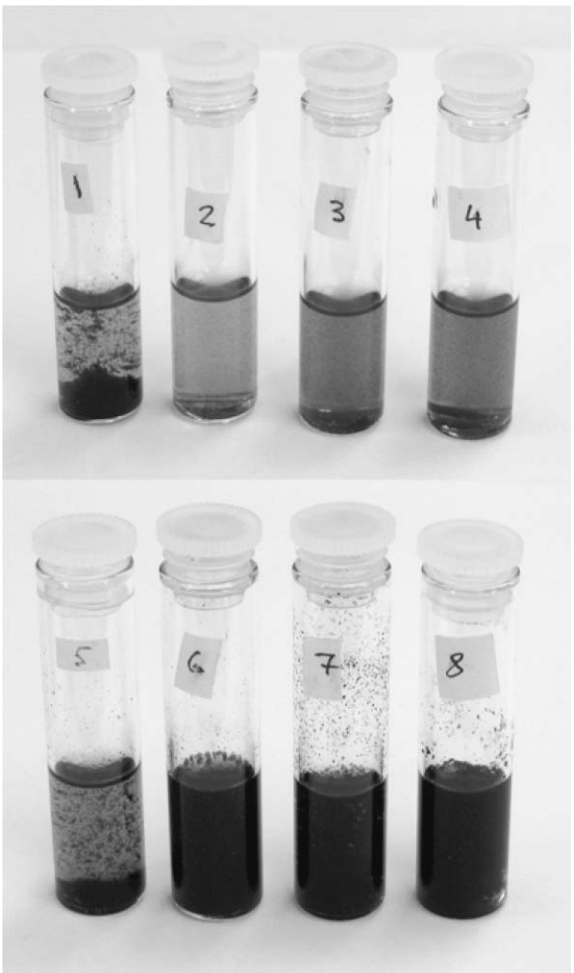


**Fig. 1** Dispersions of the different nanotube samples 15 min after 5 min of ultrasonication in isopropanol: (1) $SWNT_{ox}$, (2) $SWNT_{ox}18$, (3) $SWNT_{ox}18A$, (4) $SWNT_{ox}18C$, (5) MWNT, (6) MWNT18, (7) MWNT18A, and (8) MWNT18C.

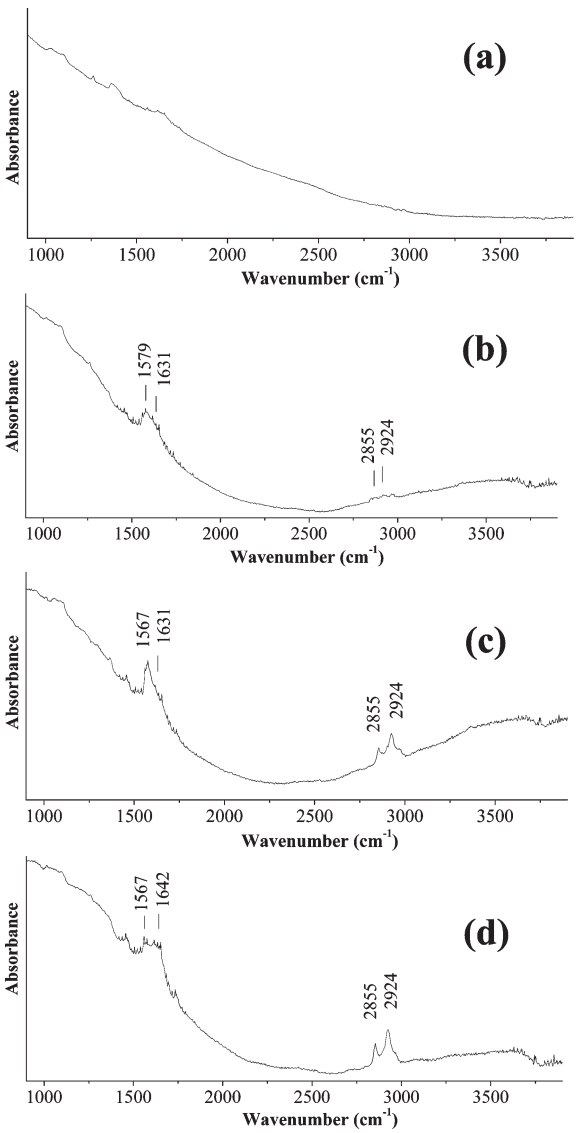


**Fig. 2** FTIR spectra (baseline uncorrected) of the oxidized SWNTs before and after their gas-phase treatment with 1,8-diaminooctane, L-alanine and ε-caprolactam: (a) $SWNT_{ox}$, (b) $SWNT_{ox}18$, (c) $SWNT_{ox}18A$, and (d) $SWNT_{ox}18C$.

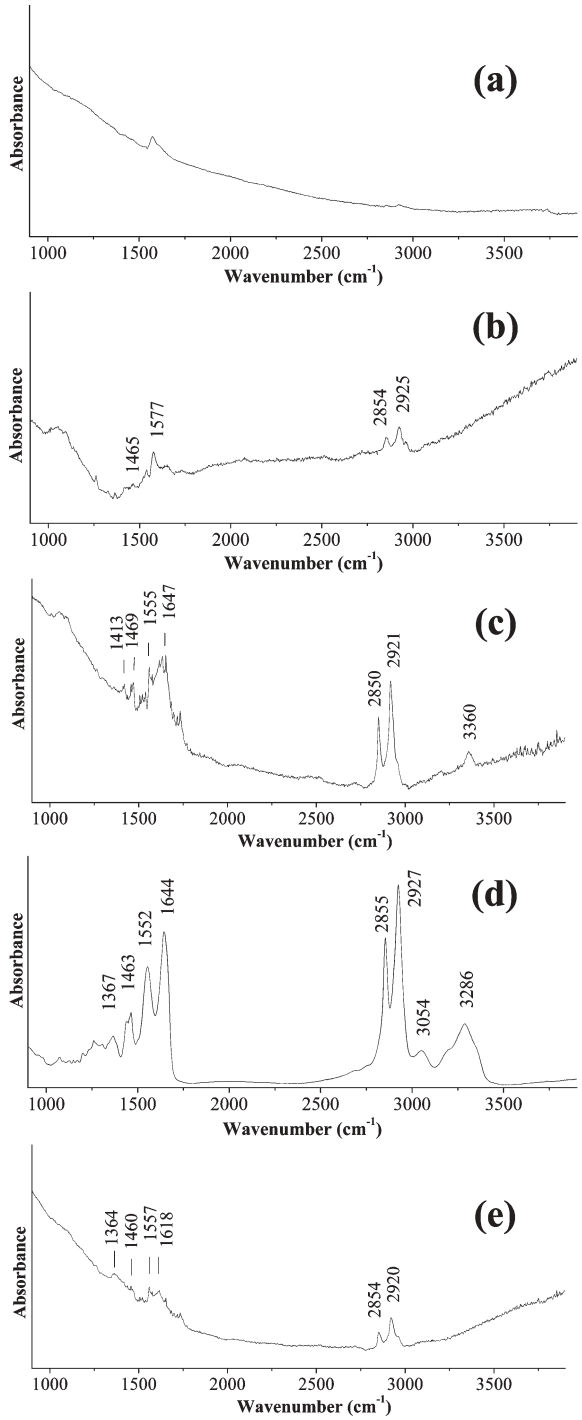


**Fig. 3** FTIR spectra (baseline uncorrected) of the pristine MWNTs before and after their gas-phase treatment with 1,8-diaminooctane, L-alanine and ε-caprolactam: (a) MWNT, (b) MWNT18, (c) MWNT18A, (d) MWNT18C, and (e) MWNTC.

(Fig. 2), whereas in the case of multi-walled derivatized nanotubes MWNT18A and MWNT18C it was clearly visible (Fig. 3).

The latter spectrum (Fig. 3d) merits special attention. All of the bands due to the organic component are so intense that the nanotube background becomes almost indistinguishable. The organic phase can be quickly identified as Nylon 6, whose IR spectra were not only studied in detail for the pure polymer,[35–37] but also reported for its composite with SWNTs.[32] This observation implies that the nanotube-bound amino groups of MWNT18 can act as an efficient initiator of ε-caprolactam polymerization from the gas phase (Scheme 1). However, the possibility exists that the sidewall defects are also capable of inducing this process. In order to prove or discard this, we performed the gas-phase treatment of pristine MWNTs with ε-caprolactam under the same conditions (evacuated and sealed vial, 160 °C, 4 h), and measured the FTIR spectrum of the nanotubes after removal of the excess ε-caprolactam by evacuation/heating. As can be seen in Fig. 3e, the formation of amide-type species to the surface of pristine MWNTs can be detected; however, the band intensity for MWNTC is roughly one to two orders of magnitude lower than in the case of MWNT18C, and hence, it is clear that the formation of Nylon 6 chains is not particularly efficient.

Because of the relatively small size of the nanotube-bound organic moieties, electron microscopy studies are not capable of detecting any substantial changes in the nanotube structure for $SWNT_{ox}18$, $SWNT_{ox}18A$, MWNT18 and MWNT18A. At the same time, Nylon 6 chains were easily seen in TEM images of MWNT18C (Fig. 4). Depending on focus, it was possible to observe their segments on the nanotube sides (when the electron beam was focused on the nanotube center), or even their long polymeric chains wrapping the nanotubes (when the beam was focused on the front or rear MWNT surface). Lower resolution SEM images (Fig. 5) showed that the polymer phase is distributed non-uniformly throughout the MWNT18C sample. While, as a whole, no evident nanotube agglomeration was observed, some globular inclusions were found (left-upper and left-middle sections in Fig. 5b).

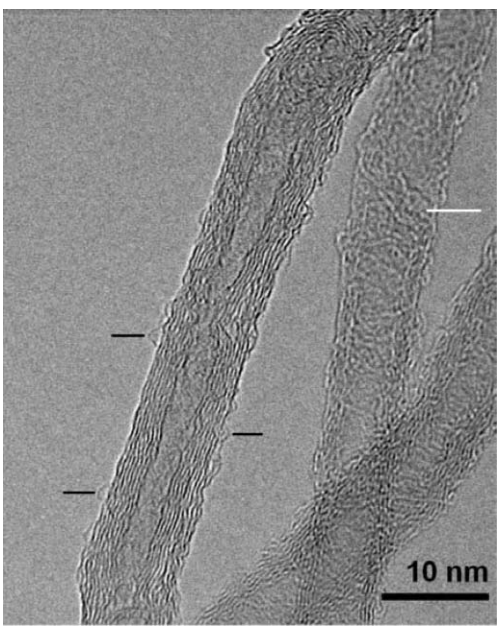


**Fig. 4** A typical TEM image of MWNT18C. The electron beam was focused on the center of the left nanotube, where segments of Nylon 6 chains are marked with black bars. The white bar points to the section where the beam focuses on the front or rear nanotube surface wrapped with polymeric chains.

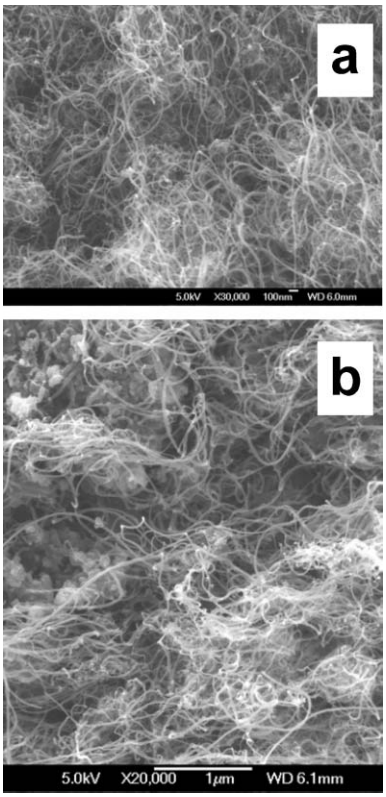


**Fig. 5** Comparison of SEM images of (a) pristine MWNT and (b) MWNT18C samples.

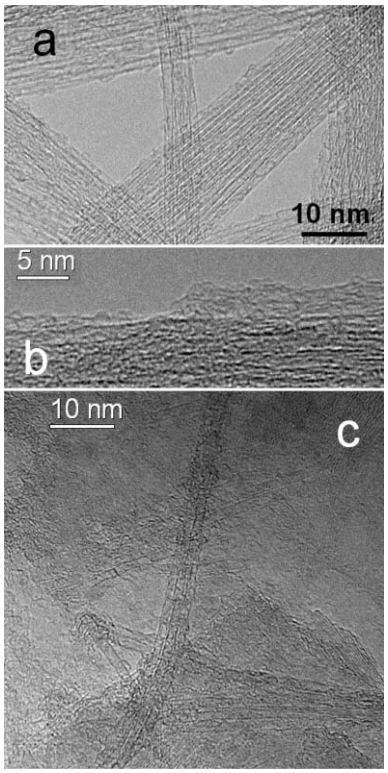


**Fig. 6** Comparison of TEM images of (a) $SWNT_{ox}$ and (b,c) $SWNT_{ox}18C$ samples: (b) amorphous material on the surface of $SWNT_{ox}18C$ bundle; (c) the nanotubes dispersed in the polymer phase.

Oxidized SWNTs assemble into large bundles of typically tens to hundreds of single nanotubes (Fig. 6). The formation of the Nylon 6 phase was detected by TEM in two different ways. In some cases the bundle structure did not noticeably change, and the polymer appeared as a separate minor phase outside the bundles (Fig. 6b). In other cases, the Nylon 6 phase dominated, acting as a solvent debundling the nanotubes, so that isolated SWNTs and thin bundles of a few nanotubes were easily distinguished (Fig. 6c). Lower-magnification SEM images (Fig. 7) also demonstrated dramatic changes in the SWNT bundle structure: while other SWNT samples looked somewhat fluffy with numerous nanotubes/thin bundles coming out of the sample (*e.g.*, $SWNT_{ox}$, Fig. 7a), the polymeric phase in $SWNT_{ox}18C$ 'glued' them together and made the samples look much denser (Fig. 7b).

On the other hand, both MWNT18C and $SWNT_{ox}18C$ became more easily dispersible in isopropanol, enabling good-quality AFM imaging (contrary to other nanotube samples studied, which remained strongly aggregated, making distinguishing the single nanotubes extremely complicated or not possible at all). The $SWNT_{ox}18C$ sample exhibited a non-uniform structure (Fig. 8a). The irregularly shaped spots observed here are due to the polymer attached mainly to SWNT terminations, which originally contained the COOH functionalities subjected to amidation with 1,8-diaminooctane, and then to the derivatization with ε-caprolactam (Scheme 1). This was not the case for MWNT18C, where the reactive defect sites were located both on the closed caps and throughout the sidewalls, giving rise to a more uniform coverage with Nylon 6 chains (Fig. 8b); the polymeric layer is a few nanometres thick, according to a simple estimate.

The organic content was estimated from TGA curves, by analyzing the total weight loss up to 500 °C. Combined TGA–DSC curves are shown for MWNT samples in Fig. 9. For

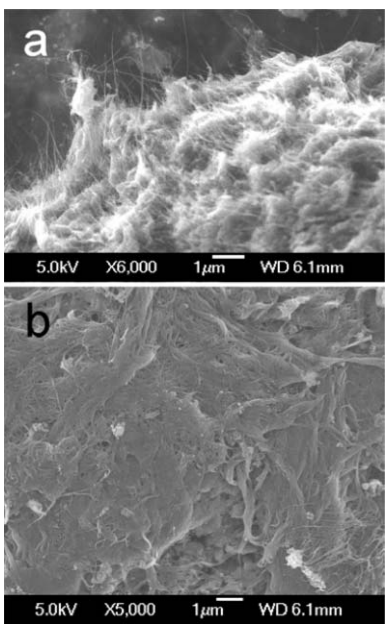


**Fig. 7** Comparison of SEM images of (a) $SWNT_{ox}$ and (b) $SWNT_{ox}18C$ samples.

 

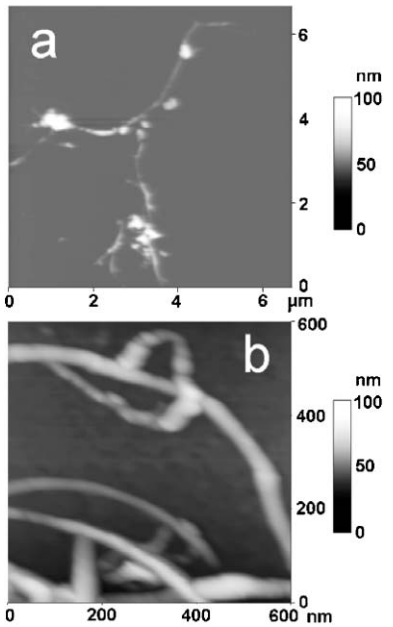


**Fig. 8** AFM images of (a) $SWNT_{ox}18C$ and (b) MWNT18C samples, deposited onto mica supports from isopropanol.

MWNT18, the weight loss due to organics barely exceeded 5%. It further increased by a few percent for MWNT18A due to the contribution of chemically attached L-alanine fragments. As was expected, the highest value of about 13% was found for the MWNT18C sample. The MWNTC sample (blank experiment, *i.e.* pristine MWNTs were directly treated with ε-caprolactam), where the formation of amide species was detected by FTIR spectroscopy (Fig. 3e), did not exhibit any substantial differences in TGA and DSC curves from those of pristine MWNTs. It is therefore clear that the presence of 1,8-diaminooctane linkers is indeed essential for the formation of Nylon 6. Besides the sharpest exothermic peak in DSC curves after 600 °C due to burning the nanotubes, the chemically modified MWNT samples exhibited a shallow peak

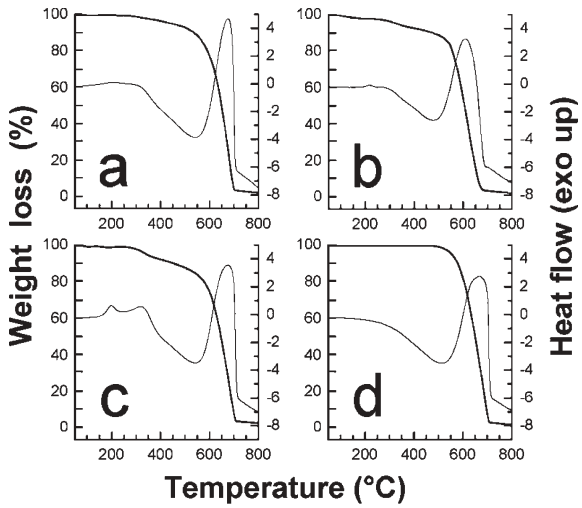


**Fig. 9** TGA (thick lines, left axis) and DSC curves (thin lines, right axis) of the nanotube samples: (a) MWNT18, (b) MWNT18A, (c) MWNT18C, and (d) MWNTC.

at 300–325 °C corresponding to thermal decomposition of the organic moieties. The MWNT18C sample had an additional important feature, namely, an exothermic peak at about 200 °C. According to recent results by Liu *et al.*,[38] who studied MWNT/Nylon 6 composites by DSC, such a peak can be indicative of a reorganization or recrystallization of the polyamide phase during the heating process.

## 3. Experimental

We used MWNTs prepared by a CVD process (97%+ purity, diameter of 10–20 nm and length of 10–50 μm) and SWNTs prepared by arc-discharge process (95%+ purity, diameter of 1–1.2 nm and length of a few hundred nm) from ILJIN Nanotech Co., Inc., Korea. 1,8-Diaminooctane, L-alanine and ε-caprolactam (all 99% purity from Aldrich) were used without additional purification. To generate carboxylic functionalities on SWNTs, and at the same time to avoid substantial cutting, the nanotubes were treated with concentrated nitric acid at *ca.* 80 °C for 30 min.

The chemical modification with 1,8-diaminooctane was performed in the same way for both $SWNT_{ox}$ and pristine MWNTs. 100 mg of the nanotubes and 50 mg of 1,8-diaminooctane were placed together in a glass vial, which was then pumped down to *ca.* $10^{-2}$–$10^{-1}$ Torr and sealed. The vial was placed into a tubular furnace and heated at 160 °C for 4 h. After cooling down, the vial was opened and placed into a Schlenk tube, where the functionalized nanotubes were heated at the same temperature and simultaneously pumped out for 1 h to eliminate the excess amine. $SWNT_{ox}18$ and MWNT18 prepared in this way were further treated with Ala and ε-caprolactam. In the latter case, the procedure was the same as that for the 1,8-diaminooctane attachment; the only difference was that the mass ratio of ε-caprolactam to nanotubes was 1 : 1. The treatment with alanine was performed in a Schlenk tube under constant pumping at *ca.* $10^{-2}$–$10^{-1}$ Torr and 160–200 °C for 1 h. The nanotubes treated in this way ($SWNT_{ox}18A$ and MWNT18A) were studied without any additional purification.

A Nicolet Magna 560 FTIR spectrometer was used to acquire infrared spectra of CNT samples deposited onto zinc selenide from ultrasonicated nanotube dispersions in isopropanol. To avoid contamination of the spectra with isopropanol bands, special precautions had to be undertaken: (a) drying of the ZnSe-deposited samples over a heating plate at 80 °C and then at ambient temperature overnight; and (b) a 30 min purge of the FTIR spectrometer with nitrogen gas. Raman spectra were recorded on a Dilor micro-Raman spectrometer with backscattering geometry equipped with a 488 nm $Ar^+$ laser and an Olympus BX40 microscope, working in a backscattered confocal arrangement; the abscissa (Raman shift) was calibrated with a silicon standard. A JEOL JSM-6500F instrument operating at 5 kV was used for scanning electron microscopic (SEM) measurements. Transmission electron microscopic (TEM) observations were performed on a JEOL 4000EX instrument operating at 400 kV. The atomic force microscope (AFM) used was a Digital Instruments (Santa Barbara, CA) Multimode SPM with a Nanoscope IIIa controller, operating in tapping mode with an 'E' scanner,

having a lateral range of 12 × 12 μm and a vertical range of 3.5 μm. Silicon probes (Nascatec GmbH model NST-NCHF-R), having a resonant frequency of approximately 320 kHz were used. The contact mode, despite its better lateral resolution, was found to be unsuitable, as it physically removed any deposits from the area being scanned. Thermogravimetric analysis (TGA) with simultaneous differential scanning calorimetry (DSC) was carried out on a Netzsch STA 449C instrument, with a heating ramp of 10 °C $min^{-1}$ to a maximum of 1000 °C and under an air flow of 100 mL $min^{-1}$.

## 4. Conclusions

Amide derivatives can be obtained on diamine-functionalized oxidized SWNTs and pristine MWNTs through a one-step direct amidation reaction, for example, with L-alanine and ε-caprolactam. The reaction takes advantage of thermal activation at 160–200 °C instead of chemical activation, employing condensing reagents like thionyl chloride or carbodiimides, avoids the use of organic solvents, and requires a few hours only for completion. In the case of ε-caprolactam, amino groups attached to the nanotubes are capable of initiating polymerization into Nylon 6, and therefore the procedure proposed opens the most direct way to CNT/Nylon 6 nanocomposites, where the two components are chemically bonded to each other.

## Acknowledgements

Financial support from the National Council of Science and Technology of Mexico (grant CONACYT-40399-Y) and from the National Autonomous University of Mexico (grants DGAPA-IN101906-3 and IN100303) is greatly appreciated. V.A.B. is indebted to the academic exchange program between the Royal Society and the Mexican Academy of Sciences. The authors are indebted to Hugo A. Sánchez Flores and Esteban Fregoso Israel for performing TGA and DSC measurements.

## References

1 V. N. Khabashesku, W. E. Billups and J. L. Margrave, *Acc. Chem. Res.*, 2002, **35**, 1087.
2 J. L. Stevens, A. Y. Huang, H. Peng, I. W. Chiang, V. N. Khabashesku and J. L. Margrave, *Nano Lett.*, 2003, **3**, 331.
3 S. Kawasaki, K. Komatsu, F. Okino, H. Touhara and H. Kataura, *Phys. Chem. Chem. Phys.*, 2004, **6**, 1769.
4 C. A. Dyke and J. M. Tour, *J. Am. Chem. Soc.*, 2003, **125**, 1156.
5 C. A. Dyke and J. M. Tour, *Chem.–Eur. J.*, 2004, **10**, 812.
6 E. V. Basiuk, V. A. Basiuk, J. G. Bañuelos, J. M. Saniger-Blesa, A. V. Mischanchuk and B. G. Mischanchuk, *J. Phys. Chem. B*, 2002, **106**, 1588.
7 V. A. Basiuk, K. Kobayashi, T. Kaneko, Y. Negishi, E. V. Basiuk and J. M. Saniger-Blesa, *Nano Lett.*, 2002, **2**, 789.
8 Y. Lin, A. M. Rao, B. Sadanadan, E. Kenik and Y. P. Sun, *J. Phys. Chem. B*, 2002, **106**, 1294.
9 E. V. Basiuk, M. Monroy-Pelaez, I. Puente-Lee and V. A. Basiuk, *Nano Lett.*, 2004, **4**, 863.
10 E. V. Basiuk, T. Y. Gromovoy, A. Datsyuk, B. B. Palyanytsya, V. A. Pokrovskiy and V. A. Basiuk, *J. Nanosci. Nanotechnol.*, 2005, **5**, 984.
11 R. Zanella, E. V. Basiuk, P. Santiago, V. A. Basiuk, E. Mireles, I. Puente-Lee and J. M. Saniger, *J. Phys. Chem. B*, 2005, **109**, 16290.
12 E. V. Basiuk, I. Puente-Lee, J.-L. Claudio-Sánchez and V. A. Basiuk, *Mater. Lett.*, 2006, DOI: 10.1016/j.matlet.2006.03.100.
13 T. Lin, W.-D. Zhang, J. Huang and C. He, *J. Phys. Chem. B*, 2005, **109**, 13755.
14 V. A. Basyuk and A. A. Chuiko, *Dokl. Chem.*, 1990, **310**, 15.
15 V. A. Basiuk and A. A. Chuiko, *J. Chromatogr., A*, 1990, **521**, 29.
16 V. A. Basyuk, *J. Anal. Chem.*, 1991, **46**, 401.
17 V. A. Basiuk and E. G. Khil'chevskaya, *Anal. Chim. Acta*, 1991, **255**, 197.
18 V. A. Basiuk and A. A. Chuiko, *J. Chromatogr. Sci.*, 1993, **31**, 120.
19 *Int. Pat. Appl.*, 2004, PCT/US2005/001310; V. N. Khabashesku, in *Extending the Life Span*, ed. K. Sames, S. Sethe and A. Stolzing, LIT Verlag Münster, Hamburg, 2005, pp. 147–152; V. N. Khabashesku, J. L. Margrave and E. V. Barrera, *Diamond Relat. Mater.*, 2005, **14**, 859; L. Zeng, L. Zhang and A. R. Barron, *Nano Lett.*, 2005, **5**, 2001.
20 A. Bianco and M. Prato, *Adv. Mater.*, 2003, **15**, 1765.
21 A. Bianco, K. Kostarelos, C. D. Partidos and M. Prato, *Chem. Commun.*, 2005, 571.
22 D. Pantarotto, J.-P. Briand, M. Prato and A. Bianco, *Chem. Commun.*, 2004, 16.
23 D. Gross and G. Grodsky, *J. Am. Chem. Soc.*, 1955, **77**, 1678.
24 V. A. Basiuk, T. Yu. Gromovoy, V. G. Golovaty and A. M. Glukhoy, *Origins Life Evol. Biosphere*, 1991, **20**, 483.
25 V. A. Basiuk, T. Yu. Gromovoy, A. A. Chuiko, V. A. Soloshonok and V. P. Kukhar, *Synthesis*, 1992, 5), 449.
26 V. A. Basiuk, T. Yu. Gromovoy, A. M. Glukhoy and V. G. Golovaty, *Origins Life Evol. Biosphere*, 1991, **21**, 129.
27 T. Yu. Gromovoy, V. A. Basiuk and A. A. Chuiko, *Origins Life Evol. Biosphere*, 1991, **21**, 119.
28 V. A. Basiuk, *Origins Life Evol. Biosphere*, 1992, **22**, 333.
29 V. A. Basiuk and R. Navarro-González, *J. Chromatogr., A*, 1997, **776**, 255.
30 W. D. Zhang, L. Shen, I. Y. Phang and T. Liu, *Macromolecules*, 2004, **37**, 256.
31 T. X. Liu, I. Y. Phang, L. Shen, S. Y. Chow and W.-D. Zhang, *Macromolecules*, 2004, **37**, 7214.
32 J. Gao, M. E. Itkis, A. Yu, E. Bekyarova, B. Zhao and R. C. Haddon, *J. Am. Chem. Soc.*, 2005, **127**, 3847.
33 L. Qu, L. M. Veca, Y. Lin, A. Kitaygorodskiy, B. Chen, A. M. McCall, J. W. Connell and Y.-P. Sun, *Macromolecules*, 2005, **38**, 10328.
34 M. Endo, S. Koyama, Y. Matsuda, T. Hayashi and Y.-A. Kim, *Nano Lett.*, 2005, **5**, 101.
35 A. Miyake, *J. Polym. Sci.*, 1960, **14**, 223.
36 I. Matsubara and J. H. Magill, *Polymer*, 1966, **7**, 199.
37 M.-B. Coltelli, M. Angiuli, E. Passaglia, V. Castelvetro and F. Ciardelli, *Macromolecules*, 2006, **39**, 2153.
38 T. X. Liu, I. Y. Phang, L. Shen, S. Y. Chow and W.-D. Zhang, *Macromolecules*, 2004, **37**, 7214.



 